The 2009 IEEE/RSJ International Conference on
Intelligent Robots and Systems
October 11-15, 2009 St. Louis, USA

Compact Magnetic Wheeled Robot for Inspecting Complex Shaped Structures in Generator Housings and Similar Environments

W. Fischer, G. Caprari, R. Siegwart, R. Moser

***Abstract*—In this paper, we present the mechanical design of a compact magnetic wheeled robot – with the goal to do inspection and vibration measurements in the housings of large generators and similar environments in power plants. After a detailed analysis of the specifications in this application, we present a new vehicle structure that allows for passing sharp concave corners – even with low friction coefficient between wheels and surface – and without using an additional active DOF. The advantages of this structure and the core parameters for its optimization are described in a quasi-static 2D calculation model. A prototype was implemented and successfully tested both in laboratory and real environments. The paper concludes pointing out the future improvements for a final industrial version.**

I. Introduction and State or the art

ROBOTS with permanent magnetic wheels combine the simple control of wheeled robots with the high mobility of climbing robots. Thus, they are the principle of choice when it comes to the inspection of complex-shaped structures that are made out of ferromagnetic steel and need an inspection robot with vertical mobility - such as generator housings, steam chests and other environments in power plants, huge ships or similar facilities.

The paper starts looking, in this section, at the alternative adhesion principles and other existing magnetic wheeled robots before analyzing the working environment and deriving the specifications. In chapter III, a model is proposed and the relative parameters are discovered. Before a conclusion, the final mechanical design and the test results are presented.

A. Alternative adhesion and locomotion principles

For achieving vertical mobility in complex-shaped environments, several adhesion principles have been developed and integrated into mobile robots [1]. Among all these principles, the adhesion with permanent magnets has several advantages: As it is a passive principle, there is no need for a permanent power supply for just staying on spot – as it is the case with electromagnets [2], active vacuum suction [3] or electrostatic adhesion [4]. Also smooth vertical walls can be climbed – even if there are no features to grasp [5] or miniature holes/ledges to place spines [6]. In contrast to robots that use artificial gecko hairs [7] or passive suction cups [8], surfaces that are slightly dirty and/or porous can also be climbed.

Compared to other locomotion principles that can be combined with magnetic adhesion, wheeled locomotion brings several advantages: Robots on magnetic wheels can better adapt to different curvatures or small surface irregularities than robots with magnets in the structure [9] or magnetic tracks [10], as there is neither a variation of the air gap towards the structure magnet nor a peel-off-effect on the tracks. Compared to robots with magnetic arms or legs [11], they do not need as many DOF – resulting in a simple and robust control.

B. Magnetic wheeled robots with high mobility to drive on corners, edges, ridges and other obstacles

Due to all these advantages, our research mainly focused on magnetic wheeled robots – leading to innovative vehicle structures that combine compact size, reasonable control complexity and impressive mobility.

In [12], we presented a robot concept that is able to move on very thin metal sheets with saturation problems and pass sharp ridges with fewer DOF than previous systems. The MagneBike [13, 14] was designed for inspecting complex-shaped pipe environments. It uses an active rotary lift mechanism for passing corners and a vehicles structure similar to a bike that allows for adapting to concave pipe curvatures that are relatively small compared to the robot itself. As this robot was only able to move relatively slow due to its high control complexity, a simplified version has been built as well [15]. However, all these prototypes were still too big for the here presented application and/or also showed some other disadvantages. A more detailed comparison against the here presented robot can be found in (II.A, II.B and III.A).

Also other research teams have developed magnetic wheeled robots with the ability to pass corners and edges. Interesting achievements in this field are an inspection robot for sewage pipes that implements a passive mechanism for

Manuscript received February 25th 2009. This work was done at the Autonomous Systems Lab within the Institute of Robotics and Intelligent Systems at ETH Zürich (www.asl.ethz.ch). It was supported by grant KTI 8435.1 EPRP-IW of the Swiss "Bundesamt für Berufsbildung und Technologie" and ALSTOM Power Services, Baden, Switzerland (www.alstom.ch).

W. Fischer is a PHD student at ETH Zürich, Tannenstrasse 3, CLA E 18, CH-8092 Zürich, Switzerland (phone: +41-44-632-2740; fax: +41 44 632 11 81 ; e-mail: wfischer@ethz.ch).

G. Caprari is a senior researcher at ETH Zürich (phone: +41 44 632 28 02; e-mail: g.caprari@ieee.org).

R. Siegwart holds the professorship at the Autonomous Systems Lab the at ETH Zürich (phone: +41-44-632-2358; e-mail: rsiegwart@ethz.ch).

R. Moser is Director R&D in the department of Inspection Technologies (PSPRI) at ALSTOM Power Service (phone: +41 56 205 65 09; e-mail: roland.moser@power.alstom.com)

corners and small steps – the "dual magnetic wheel" [16] and the "Pipe-Inspection-Robot" (PIR) [17] that can move along the outer surfaces of pipes with very complex geometry. A more detailed comparison towards the robots designed by our team can be found in our previous papers [12-15].

II. Application and Requirements

As already pointed out in the introduction, our goal was the development of a magnetic wheeled inspection robot at very small size that can bring vibration sensors into the housings of large generators in power plants.

A. Challenges for the locomotion system

Fig. 2 shows the typical geometry of such environments and points out the most difficult challenges regarding the maximum size and the shape of obstacles.

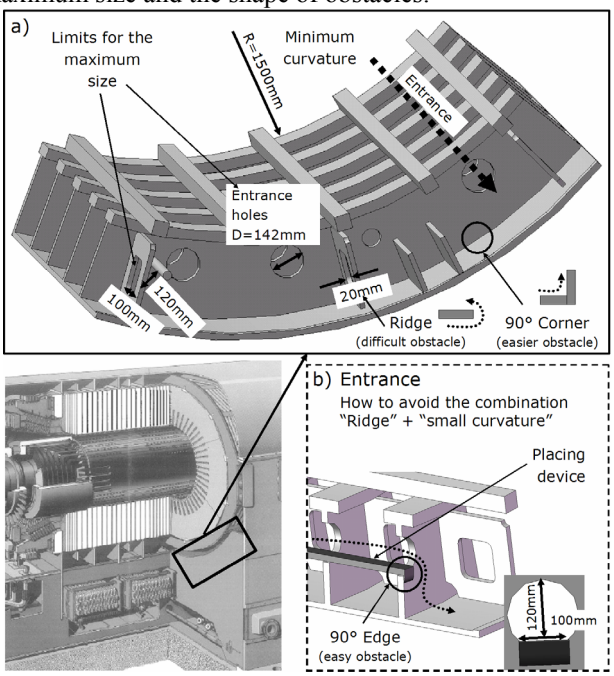

Fig. 2. a) CAD model of a typical worst-case-environment in generator back housings – with the most difficult challenges highlighted. b) Entrance method to avoid a very difficult combination of obstacles

Compared to the requirements in steam chest scenarios, for which we already developed the MagneBike [14], this application shows two significant differences in terms of size-restrictions and complexity of obstacles:

1. No need to adapt to very small curvatures (Minimum curvature radius: 1500mm instead of 100mm), but harder size restrictions (100mm x 120mm instead of a pipe with a minimum diameter of 200mm)

2. No need to pass triple steps or holes, but 90°-corners and a new worst-case-obstacle: Ridges with 20mm width.

B. Limitation on the wheel axes distance

As already pointed out in the introduction, mobile robots that are able to pass ridges in all possible inclinations of gravity normally include rather complex mechanisms for locomotion – such as magnetic legs [11] or wheels on active structures [12, 17]. Among these mechanisms, even the smallest and simplest [12] still needs 8 DOF, a minimum size of 200mm in the smallest direction and does not allow for passing 90° corners that are not part of the ridges. Downsizing one of these mechanisms with approximately factor 2 and improving its mobility at the same time seemed quite unrealistic.

Instead of following such an approach, we realized that the difficulty of an obstacle strongly depends on its size relatively to the robot. As it can be seen in Fig. 3, a ridge remains a "difficult obstacle", if the robot is relatively big compared to its size and requires a rather complex mechanism to pass it. In contrast, for a relatively small robot, it is just a combination of 90°-corners and 90°-edges. As already demonstrated in [13-16], relatively simple vehicles can pass these "easier" obstacles.

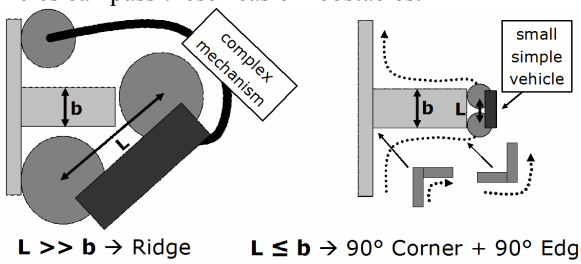

Fig. 3. Difficulty of the worst-case-obstacle (ridge with b=20mm) in relation to its size relatively to the robot

The limit condition for completely separating a "ridge" into two "edges" and two "corners" is reached, when the wheel axes distance (L) is smaller or equal than the width of the ridge (b) that is 20mm in our application.

C. Final specifications for the vehicle design

Apart from the limits concerning size and mobility on certain obstacles, also the payload had to be defined. For carrying at least a camera plus the vibration sensor, this requires 30g and a maximum space of 20x20x30mm.

To guarantee a long lifetime and a reasonable resistance against abrasion of the wheel rubber, a rather hard and resistant rubber had to be used. As such hard rubbers do not achieve as high friction as soft ones and also the surface is sometimes dirty, we defined a minimum required friction coefficient of μ=0.5.

Concerning the necessary adhesion force in the wheels, we also had to take care that the surface is often painted – with a layer up to 0.2mm thick that reduces the magnetic force.

As non-mandatory options we also defined that the robot should be able to pass the 20mm-ridges on the entrance holes with small-curvature (D=142mm) and to move on curved surfaces that can be found in steam chests [14] or other environments in power plants. This enlarges the application scope of our robot. As a cable to the robot was anyway planned for safety reasons (emergency-removal in case of a total failure) and for transmitting the signals from the vibration sensor, "power autonomy" and "wireless communication" were only put as non-mandatory options for potential other applications.

III. New vehicle structure that can passively pass corners even with low friction coefficient

As already stated in section II.B, the vehicle structures that are the closest to these specifications are the MagneBike [14], the simple 4-wheeled structure with all-wheel-traction [15] and the inspection robot for sewage pipes [16].

A. Limitations of existing vehicle structures

The MagneBike structure [14] is the most complex one, needing 5 active DOF and 5 sensors (strain gages) just for its locomotion. Due to this complexity, it was already quite a challenge to realize it at a size that allows for L=120mm. Downsizing it factor 6 seemed out of scope in this project. The vehicle structure proposed by Osaka-Gas [16] with the "dual magnetic wheel"-mechanism also had to be rejected, because this mechanism has a high risk of losing contact and falling down, when the robot has to pass corners in transitions from wall to ceiling (more detailed explanation: see [13, Section V.A]).

For this reason, the simple 4-wheeled structure with all-wheel traction [15] seemed the most promising. While downsizing it did not seem to be a difficult challenge, the security against slipping was still too low. This is because the value for the required minimum friction coefficient between wheel and surface when passing corners is still too high.

Thus, we had to find a new vehicle structure, that

- can passively roll through corners at a minimum necessary friction coefficient between wheel and surface below $\mu = 0.5$;
- is also able to pass edges;
- and is safe against losing contact and falling down in all inclinations with respect to gravity.

B. New vehicle structure with two motorized and two non-motorized pairs of magnetic wheels

As already shown in our previous paper [15], a simple 4-wheeled vehicle with all-wheel-traction requires a friction coefficient slightly above μ=0.5 for passing corners, but fulfills all the other specifications. The here presented approach for decreasing the required friction coefficient during the corner-passing-sequence is to add non-motorized extra wheels with lower magnetic force at the front and at the back of the vehicle.

For analyzing this idea and finding reasonable values for geometry and magnetic force distribution, we derived a quasi-static 2D-calculation model with the equations for force- and moment-equilibrium – similar as already done for a simpler vehicle structure [15, Fig. 2]. In this model, we point out to the characterizing equations in the worst-cases for slipping or losing contact and make proposals for reasonable values.

1) Mechanical model of a magnetic wheel

The worst-case for slipping normally occurs during a corner-passing-sequence, when a magnetic wheel is about to leave the old surface. In this case (see [15, Fig. 1, C]), the magnetic force (F_{mag}) still causes a negative reaction force (F_r=-F_{mag}), but no traction (F_t=μ*F_N) can be generated on the wheel any more, because the normal force (F_N) is set to zero (F_N=F_r+F_{mag}=-F_{mag}+F_{mag}=0).

2) Mechanical model of the entire vehicle

For our vehicle with 4 wheel pairs, there are 4 cases (see Fig. 5, a-d). For simplification, the effect of gravity was neglected (except for the transition c → d = worst-case for the risk to lose contact). This simplification was done, as the gravity force is significantly lower than the magnetic force (around 10 times in our prototype) and thus only has a minor influence on the necessary friction coefficient. Comparable calculations for a vehicle without extra-wheels can be found in [15]. In those referred calculations, the necessary friction coefficient changes from around μ = 0.5 (model without gravity) to μ = 0.6 - 0.8 (gravity force in the worst-case inclination). For the vehicle structure presented here, we assume that the effect of the "no-gravity"-simplification is comparable.

3) Calculation for the critical cases

With this 2D-model, we could formulate the equations for the force- and moment-equilibriums (Σ F in x, Σ F in y, and Σ M at P) in the critical cases and assign reasonable values to the core parameters. As a start value for the necessary friction coefficient between wheel and surface, we put μ=0.25, as this value was considered to be the extreme worst case for very dirty environments (→ future applications). As aiming for an even lower required friction coefficient would lead to an increased robot height (eq. (1)), we decided to not further optimize this value. Also the transitions between two "lift-off"-cases have been analyzed, as in these cases there can sometimes be the risk to lose contact.

a) Lift off wheel 2 (front main wheel)

Σ F in x: $F_{r1} = F_{t3}$

Σ F in y: $F_{r3} = F_{mag2}$

Σ M at P: $F_{r1} = F_{mag2} * L / a = F_{t3}$ ("Σ F in x")

$\boldsymbol{\mu_3} = F_{t3} / (F_{mag3} + F_{r3})$ (Fig. 4, A)

$= (F_{mag}*L/a) / (F_{mag3} + F_{mag2})$

$= \mathbf{L / 2a}$ (1)

With $\mu_3=\mu=0.25$ → $\boldsymbol{a/L = 2}$ (1a)

Transition a → b

Main risk: lose contact in wheel 1 (front extra wheel)

→ Need for also using magnetic wheels in the extra wheels, but with smaller magnetic force as in the main ones (F_{magS})

b) Lift off wheel 1 (front extra wheel)

In this case, slipping is not critical; as in this case both motorized wheels (2 and 3) provide traction.

Main risk: Lifting off wheel 3 (rear main wheel)

To avoid this: $- F_{r3} < F_{mag3}$ (Fig. 4, C)

Σ M at P: $F_{magS1} = - F_{r3} * e / c$

→ $F_{magS1} < F_{mag3} * e / c$

With a/L=2 ("1a") → e/c ≈ 0.5 (coming from rough approximations: c ≈ a; e ≈ L → c/e ≈ a/L)

→ **$F_{magS} < 0.5 * F_{mag}$** (2)

Design proposal: ***$F_{magS} = 0.3 * F_{mag}$*** (2a)

Transition b → c

No risk of falling: the two main wheels (wheel 2 and 3) are in contact to the surface.

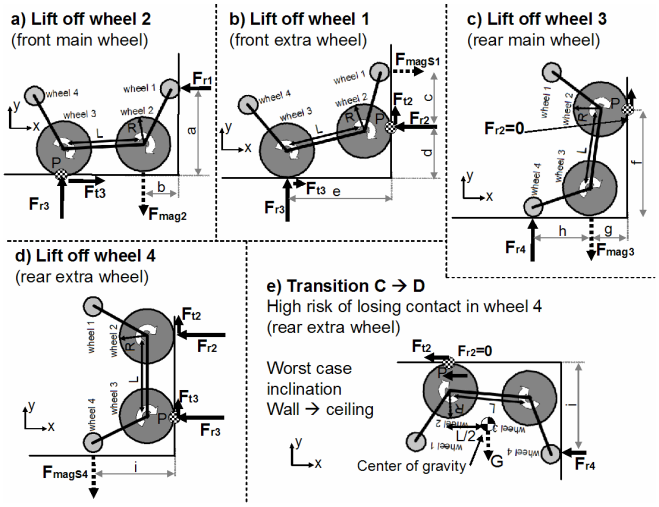

Fig. 5. Quasi-static 2D-model for calculating the corner-passing sequence of a vehicle with 2 motorized and 2 non-motorized pairs of wheels

c) Lift off wheel 3 (rear main wheel)

ΣF in x: $F_{r2} = 0$

ΣM at P: $F_{r4} = F_{mag3} * g / (g + h)$

ΣF in y: $F_{t2} = F_{mag3} - Fr4$

$= F_{mag3} * (1 - (g / (g + h)))$

$= F_{mag3} * (g + h - g) / (g + h))$

$= F_{mag3} * h / (g + h)$

$\mu_2 = F_{t2} / (F_{r2} + F_{mag3})$ (Fig. 4, C)

$= (F_{mag3} * h / (g + h)) / (0 + F_{mag3})$

$= \mathbf{h / g+h}$ (3)

$g/h = (1- \mu_2) / \mu_2$

With $\mu_2 = \mu = 0.25$ → ***$g/h = 3$*** (3a)

Transition c → d (drawing: Fig. 5, e)

Highest risk of losing contact in wheel 4 (rear extra wheel)

Traction on wheel 2 (F_{t2}) is necessary to overcome the gravity force (G), but leads to a negative reaction force on wheel 4 ($-F_{r4}$)

To avoid losing contact: $- F_{r4} < F_{magS4}$

ΣM at P: $- F_{r4} = G * (L/2) / i$

→ **$G * (L/2) / i < F_{magS}$** (4)

→ The values for i/L and for F_{magS}/G should be big enough to prevent this.

Possible with previous proposals for the core parameters:

$F_{magS} = 0.3 * F_{mag}$ (eq.(2a)) and g/h = 3 (eq. (3a))

d) Lift off wheel 4 (rear extra wheel)

For not lifting up the front main wheel (2):

ΣM at P: $F_{r2} = -F_{magS4} * i / L > F_{mag}$

With $F_{magS4} = 0.3 * F_{mag}$ (see eq. (2a))

→ **i < L** → easy to fulfill with g/h=3 (see eq. (3a))

Assumption: $\mu_2=\mu_3=\mu_{23}=\mu$

→ $F_{t2} = F_{t1} = 0.5 * F_{magS4}$

$\mu = 0.5 * F_{magS} / F_{mag}$ (5)

With $\mu = 0.25$

→ ***$F_{magS} < 0.5 * F_{mag}$*** *(Similar to eq. (2))*

C. Summary of calculation results and discussion of the parameters for the mechanical design

With this calculation model, it can easily be seen that it is possible to pass corners with a required friction coefficient of only μ=0.25 (without the effect of gravity). For comparison: a structure without these extra wheels needs μ=0.5 in similar conditions [15]). From our experience with similar robots [12-15], we assumed that including the effect of gravity, μ > 0.5 would not be reached even in the worst-case inclination. The model also helped to extract the most important design parameters (see Fig. 6) and for assigning reasonable values for a mechanical design that fulfills the specifications in our application.

1) $F_{magS} = 0.3 * F_{mag}$

A value above 0.5 * F_{mag} would bring the risk to lift off the main wheels when it is not wanted (eq. (2a)). A very low value would bring the risk to pull off the extra wheels, lose contact and fall down during the transitions when only one of the main wheels is in contact with the surface (most critical: transition c → d).

2) 2R < L < 20mm

A very short wheel axes distance (L<2R) or not enough ground clearance would bring problems on edges [13]. The limitation of L<20mm is for completely separating a 20mm-ridge into two edges (see Fig. 3).

3) Front extra wheel in a high position, but not too high
Reasonable compromise: a/L=2

The higher the distance between the front extra wheel and the ground (a) in relation to the wheel axes distance (L), the lower the required friction coefficient. However, a high value for "a/L" also increases the total vehicle height and can cause problems when small steps (<a) have to be passed (not required in the generator-application, but in steam chests). With a minimum friction coefficient of "μ=0.25", the value for "a" results to be "2L" (eq. (1a)).

4) Rear extra wheel in a low position, but not too low
Reasonable compromise: g/h=3

The lower the rear extra wheel, the lower the required friction coefficient. However, when it is too low, there is a risk to pull off the rear extra-wheel before the rear main wheel comes into contact – especially when passing from wall to ceiling (see Fig. 4, transition c → d). Again, we calculated with "μ=0.25, leading to "g/h = 3" (eq. (3a)).

D. Steering, torque transmission and free joint

For steering the robot, we decided for squid-steering, powering both wheels on each side with the same speed.

For decreasing the complexity, we decided to power the two main wheels on each side with the same motor, using spur gear transmissions. This solution was simpler to realize

at this small size than a transmission with gearbelts, worms or putting one motor per wheel.

As already suggested in [15], we also added a free joint in the structure. This passive DOF assures that all 4 powered wheels can stay in contact with the ground when edges are not passed straight or if the surface is curved. The free joint was placed perpendicular to the driving direction, as the wheels on each side are already connected with a structure that holds the spur gear transmission. For avoiding extreme movements when turning on irregular surfaces (can cause an unwanted lift-off of one wheel), we limited this free joint, to approximately +/-15°.

IV. Detailed Mechanical Design

Within the detailed mechanical design, the main goal was to achieve a maximum payload at the given short wheel axes distance that was determined by the ridges (L<20mm). At this size, we chose the strongest magnetic wheels we could get, then dimensioned motors + gears, and designed the structure around these components – according to the parameters specified in the last section and using plastic parts from a rapid-prototyping machine.

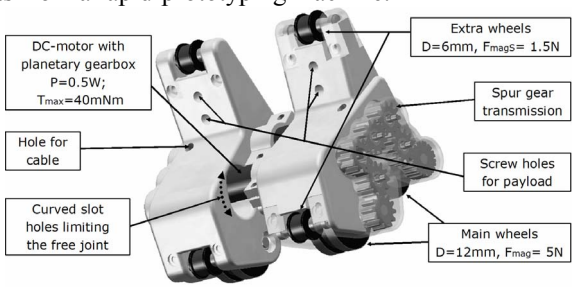

Fig. 7. Detailed mechanical design (without camera and vibration sensor)

A CAD-model of the mechanical design can be seen in Fig.7. The main wheels are made out of NdFeB35-ring magnets (Ø10/3x2mm) with steel rims on both sides (Ø12x2mm). The adhesion force (including the rubber cover) was measured to F_{mag}=5 N (per wheel) on a painted surface with a layer thickness of approximately 0.2mm and to F_{mag*}=10N on blank steel.

For increasing the friction coefficient towards the surface, we coated the rims with a thin cover of rubber (approximate thickness: 0.1mm). To achieve such a very thin but still robust cover that allows for a high friction coefficient, we did several experiments – testing different types of rubbers, molding and gluing methods. Finally, we found a relatively simple, robust and cheap solution: When gluing elastic self-adhesive tape (normally used for electric isolation) to the steel rims with cyan-acrylic glue and removing the tape after a few seconds, a very thin coating of rubber remains on the wheel. Tests showed that this coating is relatively robust against abrasion even on rusty surfaces and allows for μ=0.5-0.7, depending on how clean is the surface.

For the non-motorized extra wheels, we used smaller magnets and rims – Ø5/2x3mm ring-magnets with Ø6x0.5mm rims. With these wheels, we measured a force of F_{magS}=1.5 N=0.3* F_{mag} on the painted surface.

For calculating the required maximum torque, we used the same model as for defining the geometrical parameters. With the values for F_{mag*} and F_{magS*} (worst case here: the unpainted surfaces), the maximum torque was calculated to approximately 20mNm (without gravity effect) leading to the assumption that it would be around 30mNm in real conditions. This value can already be achieved with a geared motor of only 6mm diameter. For our prototype, we used a Maxon RE6 with 221:1 planetary gearbox (6V, 0.5W, 40mNm). For distributing this torque to both wheels, we used a 1:1 spur-gear-transmission with Teflon-gears (Mod 0.5, 12 teeth).

For the free joint between both units (necessary for better adapting to the surface), we connected them with a long 2mm-shaft in the center. To limit the movement to +/- 15°, we placed the motors (that anyway penetrate into the opposing unit) into curved slot-holes. For fixing the payload (camera + vibration sensor) two screw holes (M2) are placed on both wheel units. The total mass of the prototype is 54g (without payload).

For the first tests, the prototype was remote-controlled with bi-directional switches to change the polarization for forward- and backward movement. For the final industrial version we propose to use motors with encoders, measure the odometry and implement speed control

V. Test results with this prototype *(also see video)*

We then tested the prototype both in a laboratory test environments and in real power plant environments.

A. Mobility in the laboratory environment

In the laboratory environment, the robot moved at a speed of approximately 2m/min (no big differences if upwards, flat or downwards) and successfully passed corners, edges and curved surfaces (we tested down to D=250mm) without any problems and in all inclinations. On ridges (= double edges) we even noticed that it was possible to pass them at a thickness of only 8mm (=L-(2*R)) instead of 20mm (L). Out of this result, we realized that it is not necessary to completely separate a ridge into 2 edges; and that we can build future versions even bigger (1.5 – 2 times).

Turning and moving backwards was possible in all inclinations and also on curved surfaces. Only through corners, the robot could only pass forwards. This limitation was not seen critical, as in most environments there is enough space for turning on spot. Thus, traveling long distances backwards is not necessary.

Also the payload capability was tested. While on vertical walls, overhanging sections and corners the specified 30g could be carried easily, on edges only 15g were possible due to saturation effects on the edge that reduce the magnetic force. This corresponds to a camera with a servo for tilting it, but is perhaps not enough to also carry the vibration sensor. In a bigger version or with more expensive magnets (NdFeB60), this limitation could be solved.

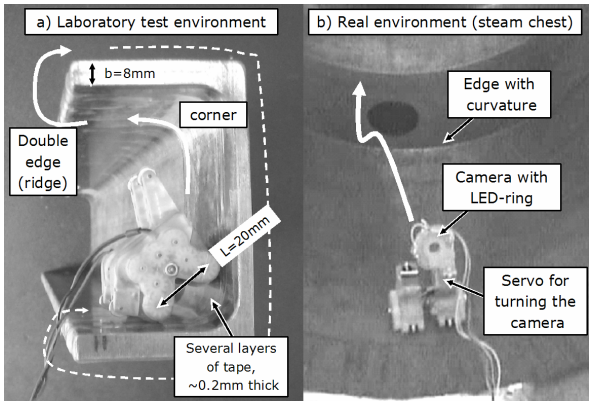

Fig. 8. Tests in a laboratory environment (a) and in a real steam chest (b) More details about these tests can be seen in the attached video.

B. *Tests in real power plant environments*

For the tests in real environments, we both tested at the first segment of a generator housing and in the steam chest environment where we had already tested the MagneBike. For these tests, we placed a standard USB-webcam and a ring of 4 LEDs on the robot. For turning, the camera, we used a servo that is normally used for small RC airplanes. The entire unit with camera, light and servo resulted in a payload of approximately 15g.

In the generator housing, the robot moved without problems. The only difficulty was to drive it with the camera-image as the only information. For this reason, future versions should also include at least an inclination sensor to provide additional information to the human operator.

Also in the steam chest, the robot passed most obstacles without problems. Only small holes of approximately 2-5mm could not always be passed. These obstacles had not been any difficulty for the relatively big MagneBike ($R_{MagneBike}$=30mm=5*$R_{robot\ in\ this\ paper}$)

From these tests we could conclude, that the current prototype is already well suited for its originally specified environment and also has potential for alternative ones.

VI. Conclusion and Future Work

In this paper, we presented a new vehicle structure that is able to move in a very narrow and complex-shaped ferromagnetic environment that could not be accessed with previous mobile robots. Its functionality is demonstrated both in calculations and real tests.

The tests showed that the prototype could pass all specified obstacles without problems and even showed a better mobility on the worst-case obstacle than we had expected: Instead of minimum 20mm, also ridges down to 8mm thickness could be passed.

Remaining challenges are to slightly improve the payload capability and to facilitate the control. These tasks will be addressed in the final industrial version, being 1.5 - 2 times bigger and allows for embedding encoders, an inclination sensor and/or other useful sensors for drive-assistance.

References

[1] D. Longo, G. Muscato, “Adhesion Techniques for Climbing Robots: State of the Art and Experimental Considerations”, Proc. of The 11th International Conference on Climbing and Walking Robots and the Support Technologies for Mobile Machines (CLAWAR), September 2008, pp. 6-28

[2] L. Fortuna, A. Gallo, G. Giudice, G. Muscato, "ROBINSPEC: A Mobile Walking Robot for the Semi-Autonomous Inspection of Industrial Plants", in Robotics and Manifacturing: recent trends in research and applications, Vol. 6, ASME PRESS New York (USA), pp. 223-228, Maggio 1996.

[3] J. Xiao, A. Sadegh, M. Elliot, A. Calle, A. Persad, H. M. Chiu, “Design of Mobile Robots with Wall Climbing Capability”, Proc. of the 2005 IEEE/ASME Int. Conf. on Advanced Intelligent Mechatronics, pp438~443, July 24-28, 2005.

[4] H. Prahlad, R. Pelrine, S. Stanford, J. Marlow, R. Kornbluh, “Electroadhesive Robots—Wall Climbing Robots Enabled by a Novel, Robust, and Electrically Controllable Adhesion Technology”, 2008 IEEE International Conference on Robotics and Automation, Pasadena, CA, USA, May 19-23, 2008

[5] C. Balaguer, A. Gimenez, CM. Abderrahim, “ROMA robots for inspection of steel based infrastructures”, Industrial Robot, Vol.29, N.3, pp. 246-251, 2002

[6] A. T. Asbeck, S. Kim, M. R. Cutkosky, W. R. Provancher, and M. Lanzetta, “Scaling hard vertical surfaces with compliant microspine array”, Int. J. Rob. Res., 25(12): 1165–1179, 2006.

[7] D. Santos, B. Heyneman, S. Kim, N. Esparza, and M.R. Cutkosky, Gecko-Inspired Climbing Behaviors on Vertical and Overhanging Surfaces, proceedings: IEEE ICRA 2008, Pasadena, May 19-23, 2008

[8] W. Brockmann, S. Albrecht, D. Borrmann, J. Elseberg, “ Dexterous Energy-Autarkic Climbing Robot”, Proc. of The 11th International Conference on Climbing and Walking Robots and the Support Technologies for Mobile Machines, September 2008, pp. 525-532

[9] J. Shang, S.Mondal, A.A. Brenner, B.Bridge, T.Sattar, “A Cooperative Climbing Robot for Melt Weld Inspection on Large Structures”, Proc. of The 11th International Conference on Climbing and Walking Robots and the Support Technologies for Mobile Machines (CLAWAR), September 2008, pp. 47-54

[10] W.Shen, J. Gu, Y. Shen, “proposed Wall Climbing Robot with permanent Magnetic Tracks for Inspecting Oil Tanks”, Proceedings of the IEEE Int. Conference on Mechatronics & Automation, Niagara Falls, Canada, July 2005

[11] J.C. Grieco, M. Prieto, M. Armada, P. Gonzales de Santos, “A Six-Legged Climbing Robot for High Payloads”, Proc. Of the IEEE Int. Conf. on Control Applications, 1-4 Sep 1998, pp. 446-450.

[12] W. Fischer, F. Tache, R. Siegwart, "Magnetic Wall Climbing Robot for Thin Surfaces with Specific Obstacles", Proc. of The 6th International Conference on Field and Service Robotics (FSR), 2007

[13] F. Tache, W. Fischer, R. Moser, F. Mondada, R. Siegwart, "Adapted Magnetic Wheel Unit for Compact Robots Inspecting Complex Shaped Pipe Structures", Proc. of The IEEE/ASME International Conference on Advanced Intelligent Mechatronics (AIM), 2007

[14] F. Tache, W. Fischer, R. Siegwart, R. Moser, F. Mondada, " Compact Magnetic Wheeled Robot With High Mobility for Inspecting Complex Shaped Pipe Structures", Proc. of The IEEE/RSJ International Conference on Intelligent Robots and Systems (IROS), 2007

[15] W. Fischer, F. Tache, G. Caprari, R. Siegwart, "Magnetic Wheeled Robot with High Mobility but only 2 DOF to Control", Proc. of The 11th International Conference on Climbing and Walking Robots and the Support Technologies for Mobile Machines (CLAWAR), September 2008, pp. 319-328

[16] Y.Kawaguchi, I.Yoshida, H.Kurumatani, T.Kikuta, and Y.Yamada, “Internal pipe inspection robot,” Proc. of the IEEE International Conference on Robotics and Automation (ICRA), 1995, pp. 857–862.

[17] T. Yukawa, H. Okano, and S. Komatsubara, “Mechanisms for the movement of piping inspection robot with magnetic elements,” in Proc. of the Sixth IASTED International Conference on Robotics and Applications (RA’05), Cambridge, USA, Nov. 2005.

Fast download of our previous papers in this research field [12-15]:
http://www.asl.ethz.ch/pub/index